Submitted to XXII International Conference on High Energy Physics
Leipzig, German Democratic Republic
July 19-25, 1984

Reference Code B17

CONF-840757--3

BNL-34932

ABSTRACT

Hard Quark-Quark Scattering with Exclusive Reactions *

Donald S. Barton, Gerry M. Bunce, Alan S. Carroll, Yousef I. Makdisi -
Brookhaven National Laboratory Upton, New York 11973

Bruce Baller, G.C. Blazey, Hans Courant, Kenneth J. Heller,
Steven Heppelmann, Marvin L. Marshak, Earl A. Peterson,
Michael A. Shupe, David S. Wahl
University of Minnesota
Minneapolis, Minnesota 55455

Stephen Gushue, John J. Russell
Southeastern Massachusetts University
North Dartmouth, Massachusetts 02747

BNL--34932

DE84 014375

We have begun a program designed to study hard quark-quark scattering with exclusive reactions, focusing on quasi-elastic two-body reactions with all possible quark flavor exchanges. Examples are $\pi^-p \to \pi^-p$, ρ^-p, $\pi^+\Delta^-$, $K^+\Sigma^-$, or $K\Lambda$. Of the two-body exclusives, only elastic scattering had been measured at such large t previous to our experiment. By comparing the relative importance of different final states, the energy dependence of the production ratios of these states, the prominence of resonances such as ρ^- over background in this region, and measuring polarizations where accessible, we have collected a large body of data on hard scattering in a completely new domain. Previously, essentially all short distance QCD tests have been for inclusive processes.

We have taken data with both negative and positive incident beam at 10 GeV/c on a hydrogen target and will present the first results, for $\pi^-p \to \pi^-p$ and ρ^-p at $\theta_{cm} = 90°$, $-t = 9$ GeV^2/c^2. The apparatus consists of a magnetic spectrometer, with Cerenkov particle identification, which selects stable charged particles (protons in this case) at high momentum near 90° in the center-of-mass. A large aperture array of PWCs observes the recoil particle or charged decay products. Cross sections are extremely low, approximately 1 nb/(GeV/c)^2 for elastic scattering. We will report on a sample of more than 1000 π^-p elastic events, and on ρ^-p, where the ρ^- decay distribution was observed.

We find a surprisingly large ρ^-p cross section in this large momentum transfer region, with ρ^-p about half the elastic cross section, and striking spin alignment of the ρ^-.

Alan S. Carroll - Speaker

*Research carried out under the auspices of the U.S.Department of Energy and the National Science Foundation.

HARD QUARK-QUARK SCATTERING WITH EXCLUSIVE REACTIONS

Exclusive two-body to two-body scattering at large momentum transfer represents a new laboratory for the study of hard scattering processes. In general, several types of quark diagrams may contribute, as shown in Figure 1 for meson-baryon scattering. Elastic scattering may proceed via any or all of the graphs, as can $\pi^- p \to \rho^- p$. A reaction such as $\pi^- p \to K^\circ \Lambda$ can not occur via pure gluon exchange or quark interchange. Others, such as $\pi^- p \to \pi^+ \Delta^-$ or $K^+ \Sigma^-$, require both annihilation and quark interchange. There are a large number of two-body exclusive reactions experimentally accessible with $\pi^\pm$ and $K^\pm$ meson beams, and each is sensitive to different mixtures of the graphs shown in Figure 1. If the quark graphs are flavor-independent, as expected for hard scattering where the asymptotic quark masses are small on the scale of the momentum transfered in the interaction, the amplitudes for each of the two-body exclusive reactions can be written in terms of the same quark scattering amplitudes, with corresponding relationships expected between the reaction cross sections.

In addition, for many possible two-body exclusive reactions polarization may be measured for a final state particle through its decay, and this can further constrain the quark amplitudes. For example, we report here on the reaction $\pi^- p^- \to \rho^- p$ where the angular distribution of the π^- from the $\rho^- \to \pi^- \pi^\circ$ decay analyzes the helicity state of the ρ^-. If the pure gluon exchange graph (Fig. 1a) were to dominate this reaction, helicity conservation at the quark level, a prediction of quantum chromodynamics, would require that the ρ^- helicity be the same as that of the incident π^-, or zero. Helicity-flip amplitudes are expected to be suppressed by a factor $m_q/\sqrt{s} \approx 10^{-3}$ for our case where $\sqrt{s} \sim 2$ GeV and we assume the asymptotically free quark mass of about 5 MeV. The other graphs, quark annihilation and interchange, can give a ρ^- with helicity ± 1.

The momentum transfer above which one can successfully apply perturbative QCD is debatable. However, many experimental phenomena indicate that an asymptotic region sets in for $p_T \geq 1.5$ GeV/c or $-t \geq 5$ GeV^2/c^2. Examples are the Q^2 dependence of the proton form factor (constant for $Q^2 > 5$)[1], that fixed angle elastic scattering follows dimensional counting predictions for $-t > 5$[2], and that elastic cross sections develop a flat central region at this value of momentum transfer.[3] For this experiment, $-t = 9$ GeV^2/c^2. Exclusive cross sections may be calculable with perturbative QCD, but the calculation requires knowledge of the wave functions and each quark must be accounted for. Farrar has developed a computer code to calculate cross sections for such reactions.[4] In addition, there are other theoretical madels for exclusive scattering.[5]

We report on an experiment performed at the Brookhaven AGS with an intense 10 GeV/c π^- beam incident on a hydrogen target. The first results, on elastic scattering and on the ρ^-p final state, will be presented. The apparatus (Figure 2) consisted of a single arm magnetic spectrometer which selected events with a positive particle with momentum greater than 5 GeV/c at 22° in the laboratory or near 90° in the π^-p elastic center of mass system. A large-aperture array of three proportional wire chambers recorded track information on the opposite side. With an event trigger for $\pi^-p \rightarrow$ positive + X, and $p_T > 1.9$ GeV/c, events were collected simultaneously for π^-p, ρ^-p, $K^+\Sigma^-$, $\pi^+\Delta^-$, and other exclusive final states. For elastic scattering at 90°, $p_T = 2.1$ GeV/c.

The spectrometer arm was located in a building which could pivot about the center of the target to select the scattering angle θ. The analyzing magnet was placed on its side so that its gap of 18" defined a small range of laboratory angles, $\Delta\theta = \pm 2.5°$. The magnet deflected positives down with a transverse kick of 0.8 GeV/c. The vertical deflection decoupled the momentum measurement from the large horizontal projection of the 1 meter long target at $\theta = 22°$. Assuming a point target, a momentum could be determined using a matrix trigger between drift cells in DWC1 and DWC2 after the magnet. We also required a matrix trigger

between scintillator hodoscope elements in HODO 2 and HODO 3, which reduced accidental triggers. All detectors downstream of the magnet were mounted on a table which was tilted to match the central momentum for elastic scattering, 8.1° for these data. Two threshold Cerenkov counters on the tilt table, one with $\gamma_{threshold} = 21.5$, the other with $\gamma_{threshold} = 9.6$, were used to distinguish between pions, kaons, and protons in the spectrometer arm. The momentum resolution of the arm, with proportional wire chambers upstream and narrow-cell drift chambers downstream, was $\Delta p/p = 0.5\%$ at 5 GeV/c.

5×10^6 events were recorded for 5×10^{12} incident pions on target. These priliminary results are based on an analysis of half the data. Most triggers were caused by the more copious lower momentum particles which were either accepted by the trigger (there was some acceptance down to $p_T = 1.4$ GeV/c), or which deflected from the magnet iron and fooled the trigger. 4% of the events on tape had a single spectrometer track with $p_T > 1.8$ GeV/c. Half the spectrometer tracks had no Cerenkov signal, indicating a spectrometer proton. Of these, 7% had a single side track which formed an acceptable vertex with the incident beam track and the track in the spectrometer arm. The momentum of each beam π^- was measured by bending the beam vertically upstream of the target, with scintillator hodoscope fingers in the beam to tag the particle position after the vertical deflection. We obtained $\Delta p/p = 1\%$ (rms) for these data, which gave Δ (missing mass)$^2 \approx .2$ GeV$^2/c^2$ for the reaction $\pi^- p \to p + X$.

We show in Figure 3 the missing mass distribution of the elastic sample, selected requiring coplanarity and opening angle cuts, and of the non-elastic events. The cuts used to select $\pi^- p \to \rho^- p$, $\rho^- \to \pi^- \pi^\circ$ are indicated. The apparent width of the ρ mass is consistent with the resolution (as seen in the elastic sample). If we assume a linearly falling background extrapolated from higher masses, there are approximately half as many $\rho^- p$ events as elastic events. Our preliminary value for the elastic cross section at 10 GeV/c, 90° CMS $-t = 9$ GeV$^2/c^2$ is $d\sigma/dt = 1$ nb/GeV$^2/c^2$, in reasonable agreement with previous work.[3]

The angular distribution of the π^- from ρ^- decay analyzes the helicity of the ρ^-. In the Gottfried-Jackson frame, after eliminating parity-violating terms, the distribution of the π^- is given by[6]

$$W(\theta,\phi) = 3/4\pi \left[\rho_{00}\cos^2\theta + (\rho_{11} - \rho_{1-1})\sin^2\theta \cos^2\phi + (\rho_{11} + \rho_{1-1})\sin^2\theta \sin^2\phi - 2\rho_{10}\sin 2\theta \sin\phi\right]$$

where θ is the polar angle from the incident π^- direction in this frame and ϕ is the azimuthal angle. ρ_{ij} is a spin-density matrix element for helicity i, j ρ^- amplitudes. A non-resonant S-wave $\pi^-\pi^\circ$ background would have an isotropic angular distribution.

In Figure 4a we show the angular distribution of events within the ρ-cut, plotting events versus $\cos\theta$ and ϕ. Figure 4b shows the scatter plot of an isotropic Monte Carlo distribution, filtered by our apparatus and event selection criteria. There are two regions where the acceptance is poor - near $\cos\theta = +1$ where the elastics have been cut out, and near $\cos\theta = -1$, $\phi = 0°$ where backward decays toward the beam line miss our side chambers. A $\sin^2\theta \sin^2\phi$ Monte Carlo distribution is shown in Figure 4c and a $\cos^2\theta$ distribution is displayed in Figure 4d. The data appear to have little $\cos^2\theta$, and show qualitivity the two lobes of the $\sin^2\theta \sin^2\phi$ distribution, indicating the presence of helicity ±1 and absence of helicity $\emptyset$ ρ^-. The higher mass data are consistent with isotropy, or non-resonant S-wave $\pi^-\pi^\circ$ background.

As remarked on in the introduction, if pure gluon exchange were to dominate (Figure 1a), helicity flip should be suppressed and a large $\cos^2\theta$ contribution would be expected. From the data, pure gluon exchange graphs appear to be unimportant. The other graphs in Figure 1, annihilation and quark interchange, may give helicity ±1 and 0. The strong preference for helicity ±1 amplitudes may imply that just one mechanism dominates and that a cancellation suppresses the helicity $\emptyset$ amplitudes. If so, then a relatively small number of two body reactions can overdetermine these amplitudes, leading to quite stringent QCD tests.

Acknowledgements:

We are pleased to acknowledge the technical support of E. Bihn, G. Grego, S. Marino and many members of the MPS Group at Brookhaven. Many members of the EP&S Division provided vital assistance in the design and construction of the experiment, particularly J. Walker and J. Mills. J. Steinbeck made important contributions. F. Paige, L. Trueman, G. Farrar and J. Soffer aided in the understanding of our results.

References

1. M.D. Mestayer, SLAC Report No. 214 (1978), unpublished.

2. S.J. Brodsky and G.R. Farrar, Phys. Rev. D11, 1309 (1975).

3. C. Baglin, et al., Nucl. [illegible] 97[illegible]); K.A. Jenkins, et al., Phys. Rev. D21.

4. G.R. Farrar, Proc. of [illegible] L[illegible] shop, edited by J.C. Allred, et al., [illegible] (1983). For discussion of exclusives and QCD, see G.P. Lepage and S.J. Brodsky, Phys. Rev. D22, 2157 (1980).

5. The Massive Quark Model, which treats effects of confinement dynamics, is discussed in a series of papers. See P. Chiappetta and J. Soffer, Phys. Rev. D28, 2162 (1983); G. Preparata and J. Soffer, Phys. Lett. 93B, 187 (1980) and Phys. Lett. 86B, 304 (1979).

6. J.D. Jackson, High Energy Physics Proc. Les Houches Summer School, 1965, editors C. DeWitt and M. Jacob (eqn.3.18).

a) 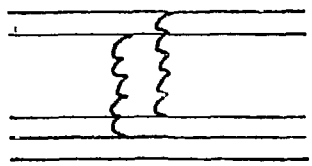 Pure gluon exchange $\pi^- p \to \pi^- p, \rho^- p$.

b) 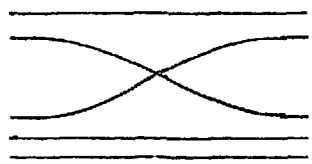 Quark interchange.

c) 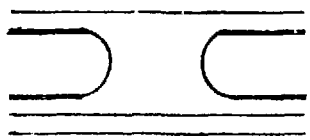 Annihilation $\pi^- p \to \Lambda K$.

d) 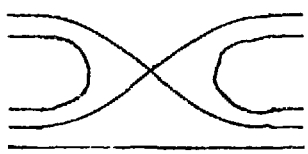 Annihilation and interchange $\pi^- p \to K^+ \Sigma^-, \pi^+ \Delta^-$.

Figure 1. Quark diagrams for meson-baryon exclusive scattering. Example reactions for the diagrams are shown. The reactions listed in (a) can proceed via diagrams (b), (c), (d). Similarly, $\pi^- p \to K\Lambda$ can proceed via (d).

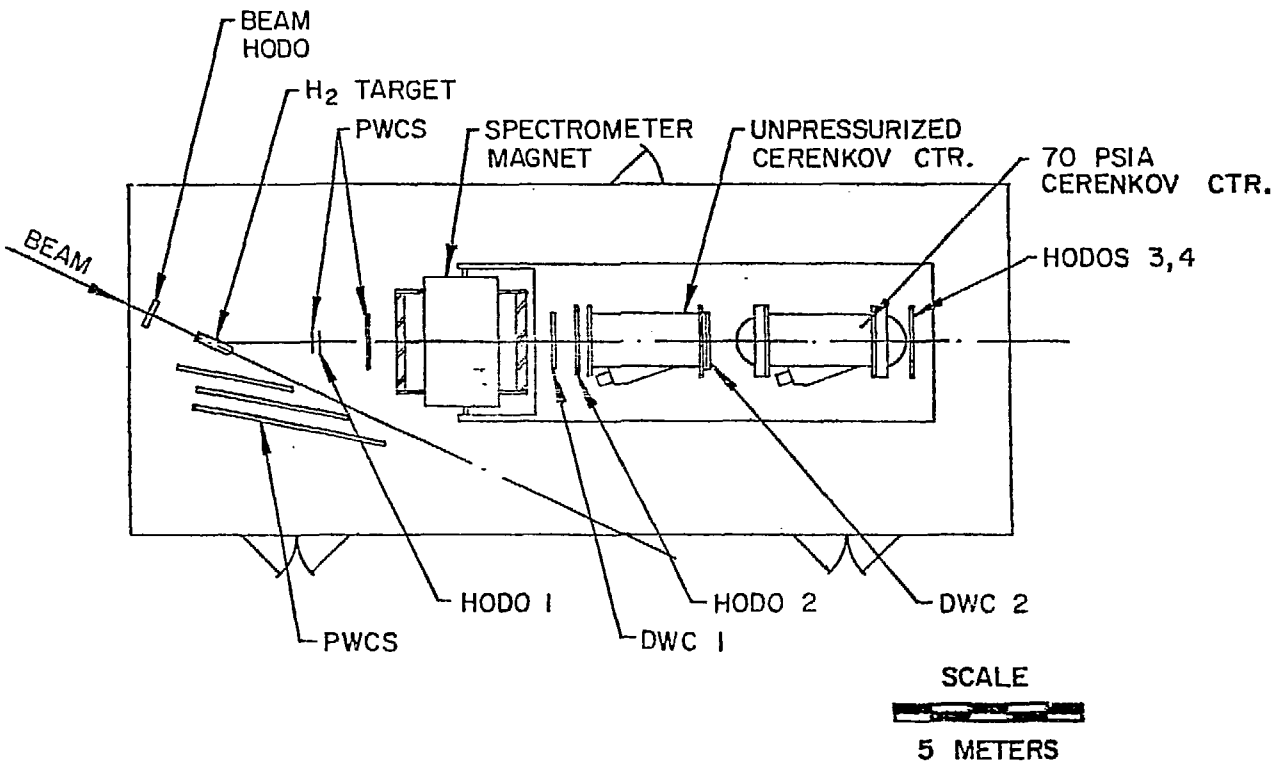

Figure 2. Plan view of experimental apparatus for measuring exclusive reactions.

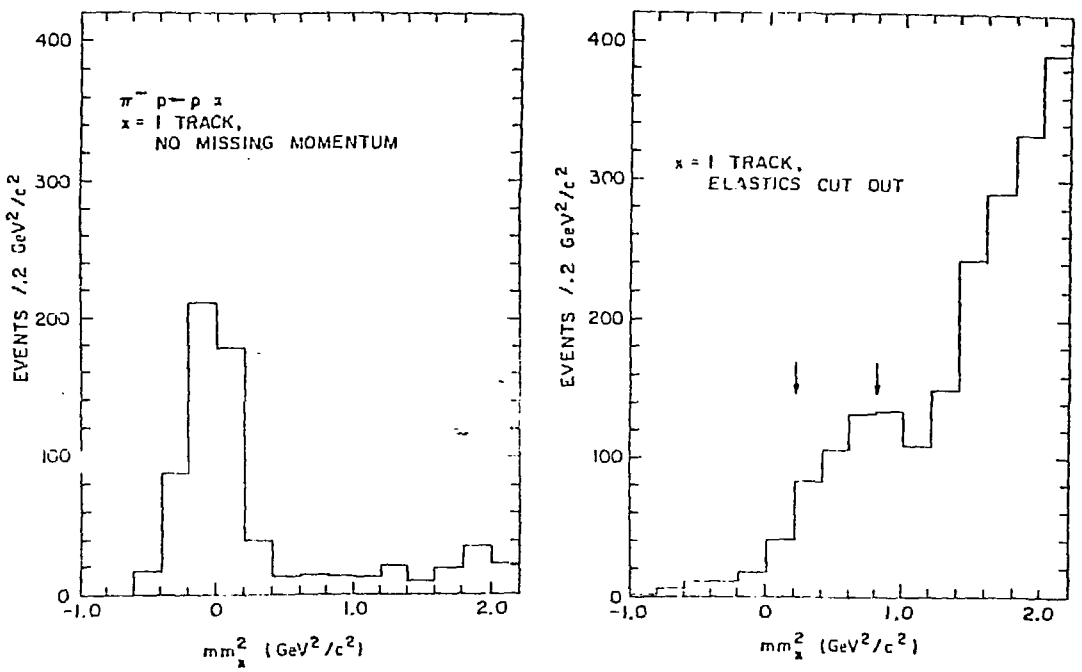

Figure 3. Mass^2(X) for $\bar{p}$ p + X at 90^o CMS, for cuts selecting elastics, and for elastics removed. Ref. 21.

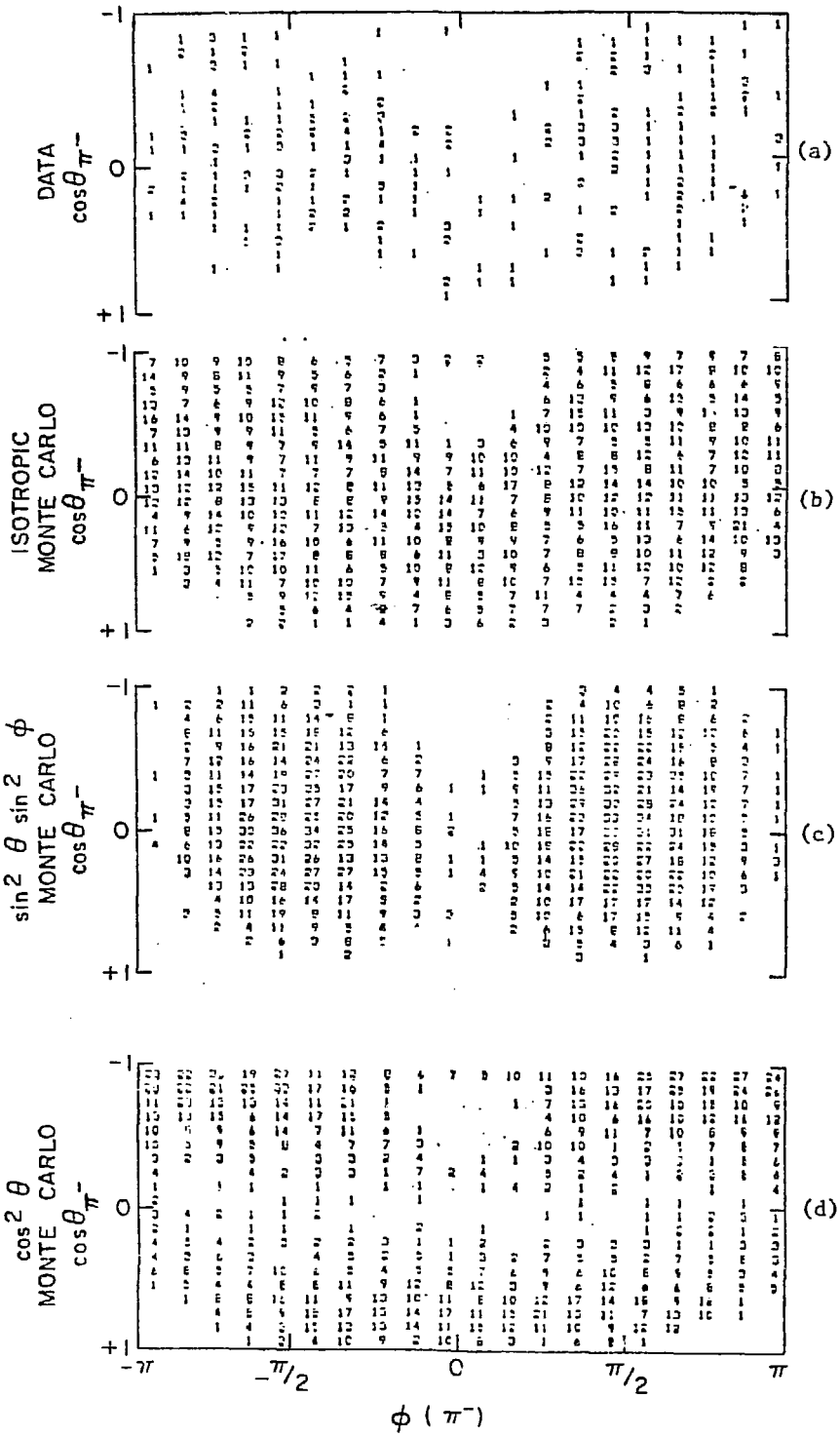

Figure 4. Scatterplots vs. cos θ and φ, the decay angles of the π^- and $\rho^- \to \pi^-\pi^0$ decay, for data and three Monte Carlo distributions.